OKU Fen Bilimleri Enstitüsü Dergisi
6(1): 35-51, 2023

OKU Journal of The Institute of Science and Technology, 6(1): 35-51, 2023

Osmaniye Korkut Ata Üniversitesi
Fen Bilimleri Enstitüsü
Dergisi

Osmaniye Korkut Ata University
Journal of The Institute of Science
and Technology

Bakır ve Pirinç Elektrot ile EDM Yönteminde Soğuk İş Takım Çeliği İşlemede MRR, EWR ve KERF Analizi

Ferhat CERİTBİNMEZ[1*], Elif Simay GÖKKAYA[2], Erdoğan KANCA[3]

[1]Haier Europe, Candy - Hoover Group, Research and Development Center, 26010, Eskişehir, Türkiye
[2,3]Iskenderun Technical University, Department of Mechanical Engineering, 31200, Hatay, Türkiye

[1]https://orcid.org/0000-0002-5615-3124
[2]https://orcid.org/0000-0002-6283-4903
[3]https://orcid.org/0000-0002-7997-9631
*Sorumlu yazar: ferhatceritbinmez@gmail.com

Araştırma Makalesi

Makale Tarihçesi:
Geliş tarihi: 26.01.2022
Kabul tarihi:20.06.2022
Online Yayınlanma: 10.03.2023

Anahtar Kelimeler:
EEİ
TKO
EAO
Kerf
Sleipner

ÖZ

Bu çalışmada, 60-62 HRC sertliğe sahip Sleipner soğuk iş takım çeliğine EEİ'de bakır ve pirinç elektrotlar'la üç farklı akım değeri (50, 25, 12,5 A), üç farklı ark süresi (3, 6, 9 µs) ve bekleme süreleri (4, 6, 8 µs) kullanılarak delikler delinmiş, bu çalışma parametrelerinin operasyon sürelerine, talaş kaldırma oranına (TKO) ve elektrot aşınma oranına (EAO), işlenen parçaların delik giriş-çıkış çaplarına, iş parçası ve elektrot üzerindeki kerf'e etkileri analiz edilmiştir. Yapılan analizler neticesinde, bakır elektrot kullanımında TKO pirinç elektrot kullanımına göre ortalama %311,25 artarken, EAO ve işleme süresi sırasıyla %42,01 ve %38,46 oranında azalmıştır. İş parçası ile elektrot arasındaki kıvılcımlanmanın ve termal etkilerin artması TKO'nun artması ve işleme süresinin azalmasını sağlamıştır. Farklı işleme parametreleriyle bakır ve pirinç elektrot kullanımında delinen deliklerin giriş çaplarının çıkış çaplarından büyük olduğu görülmüş, aşınan elektrotlar sebebiyle debris tahliyesine bağlı olarak düzensiz bir kerf oluşumuna rastlanmıştır.

MRR, EWR and KERF Analysis in Cold Work Tool Steel Machining in EDM Method by Copper and Brass Electrode

Research Article

Article History:
Received: 26.01.2022
Accepted: 20.06.2022
Published online: 10.03.2023

Keywords:
EDM
MRR
EWR
Kerf
Sleipner

ABSTRACT

In this study, holes were drilled on the Sleipner cold work tool steel with a hardness of 60-62 HRC by copper and brass electrodes using three different current values (50, 25, 12.5 A), pulse on times (3, 6, 9 µs) and pulse off times (4, 6, 8 µs) parameters in the EDM method; the effects of these working parameters on machining times, material removal rate (MRR), electrode wear rate (EWR), the hole inlet-outlet diameters of the machined parts, the kerf on workpiece and electrode were analyzed. As a result of the analyzes made, in the use of copper electrodes, the MRR increased by 311.25% on average compared to the use of brass electrodes, while the EWR and machining time decreased by 42.01% and 38.46%, respectively. The increase in sparking and thermal effects between the workpiece and the electrode resulted in an increase in the MRR and a decrease in the machining time. In the use of copper and brass electrodes with different processing parameters, the inlet diameters of the drilled holes were found to be larger than the outlet diameters as well as an

irregular kerf formation was observed due to debris evacuation due to worn electrodes.

To Cite: Ceritbinmez F, Gökkaya ES., Kanca E. Bakır ve Pirinç Elektrot ile EDM Yönteminde Soğuk İş Takım Çeliği İşlemede MRR, EWR ve KERF Analizi. Osmaniye Korkut Ata Üniversitesi Fen Bilimleri Enstitüsü Dergisi 2023; 6(1): 35-51.

1. Introduction

Electro discharge machining (EDM) is a method of removing metal from the electrically conductive workpiece by thermal effects by using copper, brass or similar electrode material in a dielectric environment (Dhanabalan et al., 2015; Payal et al., 2008; Pavan and Sateesh, 2021). In this method, the workpiece melts and evaporates due to the high temperature created by the rapid electrical discharges that occur between the electrode (cathode) and the workpiece (anode). As a result of these repeated processes, the material removal is completed without contact so that the electrode form is discharged on the workpiece (Azad and Puri, 2012; D'Urso et al., 2016; Niamat et al., 2019; Quarto et al., 2020). The non-contact and thermal processing properties of this method enable high-hardness materials, which are not possible to be processed by conventional methods, to be easily processed with this method (Akbulut and Kürşad, 2020; Shu et al., 2006). In this method, the electrode material used during material removal from the workpiece also wears off a little, which directly affects the machining time, metal removal rate and electrode wear rate. For these reasons, the mechanical, physical and chemical properties of the electrodes used in the EDM process are very important. In addition, the EDM processing parameters selected with the electrodes affect the process quality (Ceritbinmez and Yapıcı, 2021). Mahajan et al. investigated EDM machinability of high strength, temperature resistant steels by copper, brass, graphite, copper tungsten etc. electrodes. They reported that the material removal rate of the copper electrode was higher than that of the brass electrode as well as the wear rate of the brass electrode was higher than the copper electrode due to the thermal conductivity and melting point of the copper electrode are higher than the brass electrode (Mahajan et al., 2018). Sahu ve Mahapatra used copper, brass and AlSi10Mg RP as electrode material also EDM-30 as dielectric fluid in the processing of titanium alloy and AISI 1040 steel by EDM method. The effects of machining parameters such as current and pulse on time on the average surface roughness of the machined surfaces, surface crack density, white layer thickness and microhardness of the white layer were investigated by them. As a result of scanning electron microscope to observe surface cracks and Gray-TOPSIS method for analysis of optimum parameters, they reported that the best surface properties were obtained in the use of AlSi10Mg RP electrodes at low current and arc duration processing parameters (Sahu ve Mahapatra, 2020). Nas et al. used copper and graphite electrodes with processing parameters such as current values (10, 20, 30 A), three different pulse on times (100, 200, 300 μs) and pulse off times (10, 20, 30 μs) parameters to remove chips from AISI 1.2738 material in the EDM method. They tried to determine the ideal parameters for the lowest surface roughness by using the obtained data in the Taguchi Orthogonal Array Design L54 statistical method. As a result of the analysis, the most effective parameters on the surface roughness were determined as current, pulse on time, pulse of time and electrode material type, respectively. The lowest average surface roughness values were calculated as 4.73 μm by selecting the Ton 300 μs, Toff 30 μs and 10 A parameters in the use of copper electrodes, and as 4.35 μm by selecting the Ton 100 μs Toff 10 μs and 20 A parameters in the use of graphic electrodes (Nas et al., 2018). Joshi et al. investigated the processing of EN8 mold steel using copper electrodes in the EDM method and the effects of machining parameters on the roughness of the machined surfaces. They emphasized that the electrode wear rate was proportional to the material removal rate at high values of the machining parameters (Joshi et al., 2020). Mouralova et al. examined the corner and edge wear of the electrodes under electron microscope by removing chips from 1.2363 and 1.2343 ESR steels with different machining parameters using copper and graphite electrodes in the EDM method. They also investigated the wear rate of the electrodes used, the topography and surface morphology of the processed samples. They reported that there was less wear in the use of graphite electrodes, and a more precise shape and size was obtained due to the preservation of the electrode form (Mouralova et al., 2020).

In this study, chips were removed from Sleipner Cold Work Tool Steel with chromium-molybdenum-vanadium alloy with good wear resistance, high compressive strength and high hardness value by EDM method using Cupro MAX brand copper and Cuprass 3 brand high strength special brass alloy electrodes. In this context, the effects of different processing parameters on key performance outputs such as MRR, EWR, KERF and processing time were determined by analytical measurements and macro analysis. In addition, copper and brass electrode performances were evaluated and reported. The results from this article have the potential to be an invaluable reference for quality EDM applications with the best MRR, EWR, Kerf and machining time.

2. Materials and Methods

2.1. Workpiece Material

In this study, cold work tool steel Uddeholm Sleipner, which is increasingly used in industry, was chosen as workpiece. This steel is a general purpose cold work tool steel with chromium-molybdenum-vanadium alloy, high hardness and wear resistance (Kirkhorn et al., 2012; Pantazopoulos et al., 2006). Technical specifications are provided by Alseko Metal company with heat treatment; Its chemical components and mechanical properties are given in Tables 1 and 2, respectively. The dimensions of the workpiece used in the experiments were 80 x 80 x 3 mm, and these samples were sliced using a WEDM machine from a billet of 250 x 300 x 80 mm.

Table 1. Sleipner chemical component (Uddeholm, 2022)

Carbon (% C)	Silicium (% Si)	Manganese (% Mn)	Chrome (% Cr)	Molibden (% Mo)	Vanadium (% V)	Iron (% Fe)
0.9	0.9	0.5	7.8	2.5	0.5	Remnant

Table 2. Sleipner Mechanical Properties (Uddeholm, 2022)

Hardness (HRC)	Thermal conductivity (W/m•°C)	Specific heat capacity (J/kg•°C)	Modulus of elasticity (kN/mm²)	Coefficient of thermal expansion	Density (g/cm³)
60-62	20-25	460	205	12.7x10-6	7.73

2.2. Electrode Materials

In this study, Cupro MAX brand copper electrode alloyed with chromium and zirconium, which was supplied by Sağlam Metal, was used. The chemical components and mechanical properties of this material are given in Tables 3 and 4, respectively.

Table 3. Cupro MAX chemical components (Sağlam Metal, 2022)

Chromium (% Cr)	Zirchoniun (% Zr)	Other (%)	Copper (% Cu)
0.5-1.2	0.03-0.3	Maks.0.2	Remnant

Table 4. Cupro MAX Mechanical Properties (Sağlam Metal, 2022)

Hardness (HB)	Tensile Strength (N/mm²)	Yield Strength (N/mm²)	Moduls of Elasticity (GPa)	Elongation (%)	Density (g/cm³)
135-170	400-500	320-410	122	18	8.9

Table 5. Cupro MAX Physical characteristics (Sağlam Metal, 2022)

Electrical Conductivity (MS/m)	Thermal Expansion Coefficient (10-6/K)	Thermal Conductivity (W/mK)	Density (g/cm³)
45	17	320	8.9

Cupro MAX physical properties are also listed in Table 5. The electrodes supplied from the supplier in the form of rods were turned on a lathe to measure Ø 8 mm in diameter and 20 mm in length as shown in Figure 1. In order to connect these electrodes to the electrode holder on the EDM bench, M5x10 threads were drilled on the back side of the electrode. All electrodes were manually connected to the electrode holder individually before the experiments.

(a) (b)

Figure 1. Turned electrodes prepared for EDM: **(a)** Copper **(b)** brass

In this study, Cuprass 3 brand high strength special brass alloy belonging to the manganese bronze family was used in order to discuss the effects of the electrode material type on the process quality and machining time. This material was supplied from Sağlam Metal Company and its chemical, mechanical and physical properties are given in Tables 6, 7 and 8, respectively.

Table 6. Cuprass 3 chemical components (Sağlam Metal, 2022)

Aluminium (% Al)	Iron (% Fe)	Manganese (% Mn)	Zinch (% Zn)	Copper (% Cu)
3-7	1.5-4	2.5-5	Kalan	60-67

Table 7. Cuprass 3 Mechanical Properties (Sağlam Metal, 2022)

Hardness (HB)	Tensile Strength (N/mm²)	Yield Strength (N/mm²)	Moduls of Elasticity (GPa)	Elongation (%)	Density (g/cm³)
180-225	820	460	105	14	7.7

Table 8. Cuprass 3 Physical characteristics (Sağlam Metal, 2022)

Electrical Conductivity (MS/m)	Thermal Expansion Coefficient (10-6/K)	Thermal Conductivity (W/mK)	Density (g/cm³)
5	22	36	7.7

2.3. Machining Method

Furkan Brand 50 Ampere EDM (electric discharge machining) machine was used for the experiments. In the selection of the experimental parameters, the machine safe operating parameter range was taken as a reference. In addition, the best reference values obtained as a result of industrial applications were selected. In order to evacuate the sawdust between the electrode and the workpiece, Eralube brand dielectric liquid was sprayed by means of spiral metal hoses and the erosion process was carried out under dielectric liquid as shown in Figure 2. Before erosion, the dielectric liquid was sprayed with spiral metal hoses in a way to completely submerge the workpiece in the dielectric liquid, and it was evacuated from the environment after the erosion process.

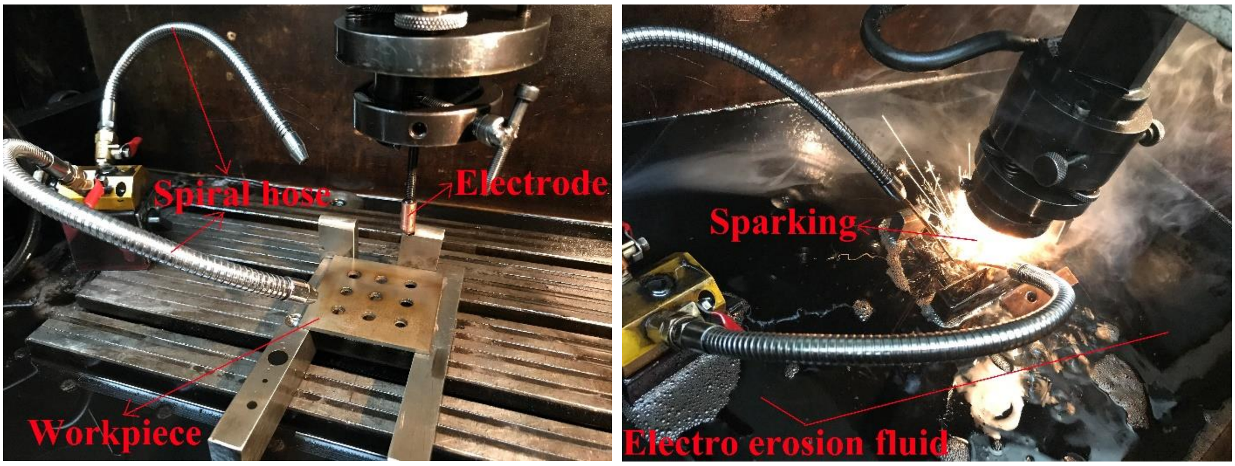

(a) (b)

Figure 2. Erosion process on Furkan EDM machine: **a** Erosion onset, **b** Erosion under dielectric liquid

2.4. Material Removal Rate (MRR) Calculations

The equality shown in Equation (1) was used to calculate the effects of different machining parameters on the MRR (material removal rate) (Kuppan et al., 2008; Rajesha et al., 2012; Soydan et al., 2020). The amount of abraded material was determined by weighing the workpiece before and after each experiment on a balance with a sensitivity of 0.001 g. In addition, each test period was recorded with the help of a chronometer and used in the calculation of the MRR.

$$MRR\left(\frac{g}{min}\right)=\frac{Initial\ weight\ of\ material-final\ weight\ of\ material}{Machining\ Time} \quad (1)$$

2.5. Electrode Wear Rate (EWR) Calculations

Electrode wear rates were determined using Equation (2) by proportioning the weight of each electrode material used in the experiments before and after machining to the processing time (Maan et al., 2018; Raj et al., 2020).

$$EWR\left(\frac{g}{min}\right)=\frac{Initial\ weight\ of\ electrode-final\ weight\ of\ electrode}{Machining\ Time} \quad (2)$$

2.6. Kerf Measurements

After the workpieces were drilled with electrodes, the kerf taper angle was calculated using the Equation (3), taking into account the hole inlet and outlet dimensions. In this equation, the hole entrance dimensions and the size of the electrode bodies (a); hole outlet, base, and electrode tip dimensions (b); hole depth and electrode processing area dimensions were calculated as *t* as shown in Figure 3 (Skrabalak et al., 2018).

$$Kerf\ Taper\ Angle\ (T)=Arctan\left(\frac{a-b}{2.t}\right) \quad (3)$$

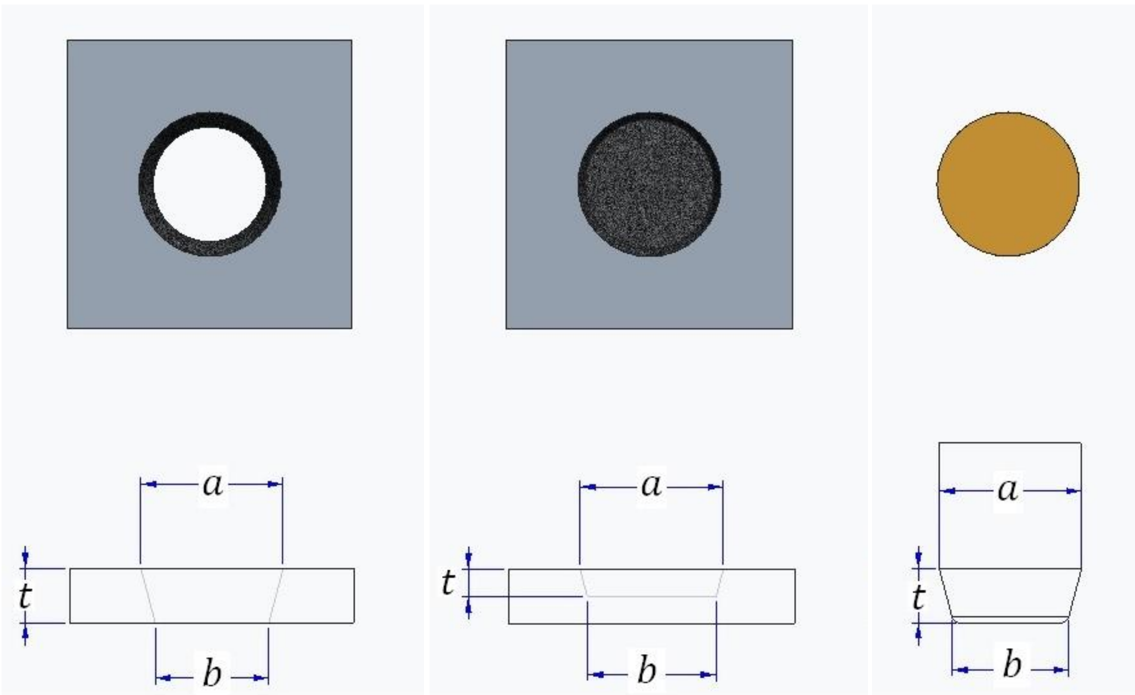

(a) (b) (c)

Figure 3. Measurement description of kerf taper angle: (a) through hole, (b) blind hole, (c) electrode tip

Hole entry size (a), hole exit size (b) and hole depth (t) of workpieces drilled with EDM were detected using a Mitutoyo digital caliper with a measurement accuracy of 0.01 mm. In the kerf measurements of the workpiece that was not drilled through, the diameter at the bottom of the blind hole was taken into account as the hole exit size as shown in Figure 3b. In the measurements made, it was determined that there were dimensional differences in the inlet and outlet regions of the material processed with EDM, therefore, a kerf conical angle formed on the electrodes. To detect these differences, measurements were made using Mitutoyo digital micrometers with a measurement accuracy of 0.001 mm from the ends and body parts of the electrodes, as shown in Figure 4 (Ceritbinmez and Kanca, 2021).

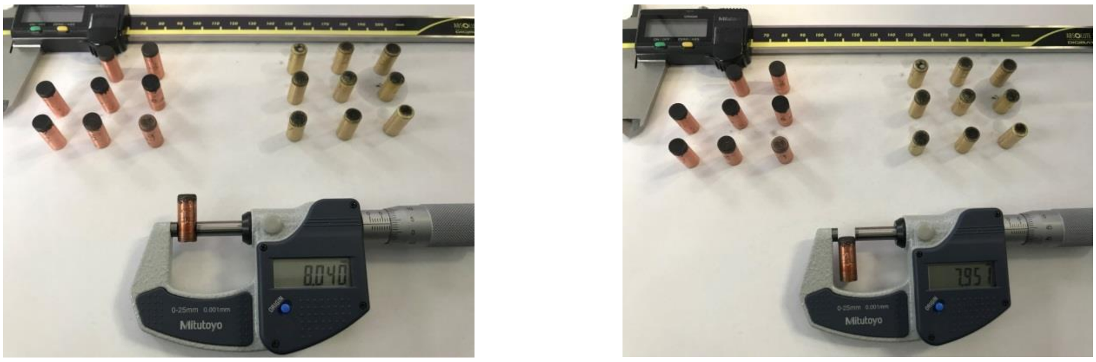

(a) (b)

Figure 4. Electrode Kerf measurement: (a) Body measurement, (b) Tip measurement

It was observed that the diameters of the tip and body parts were different from each other due to the wear on the treated parts of the copper and brass electrodes used in the EDM, and the kerf angle was formed due to the abrasions on the tip parts.

3. Results and Discussion

The experimental data and the results obtained using different processing parameters are listed in Tables 9 and 10 according to the use of copper and brass electrodes. It was observed that the processing time, MRR, EWR and kerf angles changed with the change of selected discharge current, pulse on-off time and electrode types.

Table 9. EDM operating parameters and analysis results (Copper electrode)

Test No	Discharge Currents (A)	Servo Voltage (V)	Pulse On Times (µs)	Pulse Off Times (µs)	Machining Time (min)	MRR (g/min)	EWR (g/min)	Kerf (degree)	
								Workpiece	Electrode
1	50	60	6	4	2	0.640	0.326	4.10	0.85
2	25	60	6	4	3	0.413	0.149	2.77	0.46
3	12.5	60	6	4	6	0.209	0.033	1.34	0.27
4	25	60	9	8	3	0.438	0.119	1.91	0.57
5	25	60	9	6	4	0.310	0.078	2.86	0.07
6	25	60	9	4	4	0.328	0.078	2.10	1.58
7	25	60	9	6	4	0.321	0.060	2.67	0.39
8	25	60	6	6	5	0.254	0.015	2.67	0.48
9	25	60	3	6	25	0.050	0.024	1.00	0.60

Table 10. EDM operating parameters and analysis results (Brass electrode)

Test No	Discharge Currents (A)	Servo Voltage (V)	Pulse On Times (µs)	Pulse Off Times (µs)	Machining Time (min)	MRR (g/min)	EWR (g/min)	Kerf (degree)	
								Workpiece	Electrode
1	50	60	6	4	4	0.162	0.329	2.95	0.55
2	25	60	6	4	5	0.088	0.281	3	2.26
3	12.5	60	6	4	7	0.071	0.171	0.72	0.41
4	25	60	9	8	12	0.080	0.071	1.25	0.31
5	25	60	9	6	15	0.056	0.072	2	0.24
6	25	60	9	4	17	0.045	0.067	1.94	0.15
7	25	60	9	6	13	0.074	0.084	4.34	0.84
8	25	60	6	6	4	0.106	0.368	2.83	0.31
9	25	60	3	6	14	0.042	0.082	1.97	0.40

EDM is an electro-thermal machining process. Here, the electrical energy is used to create an electric spark (arc) and as a result, the chips are removed with the thermal energy (Abhishek et al., 2017). In the case of different processing parameters and especially high current usage, different sizes of point melting and evaporation can occur on the processed surfaces. The energy transmission required for this melting and evaporation is provided with the help of the electrodes used. The treated ends and edges of the copper and brass electrodes used in this study are shown in Figure 5.

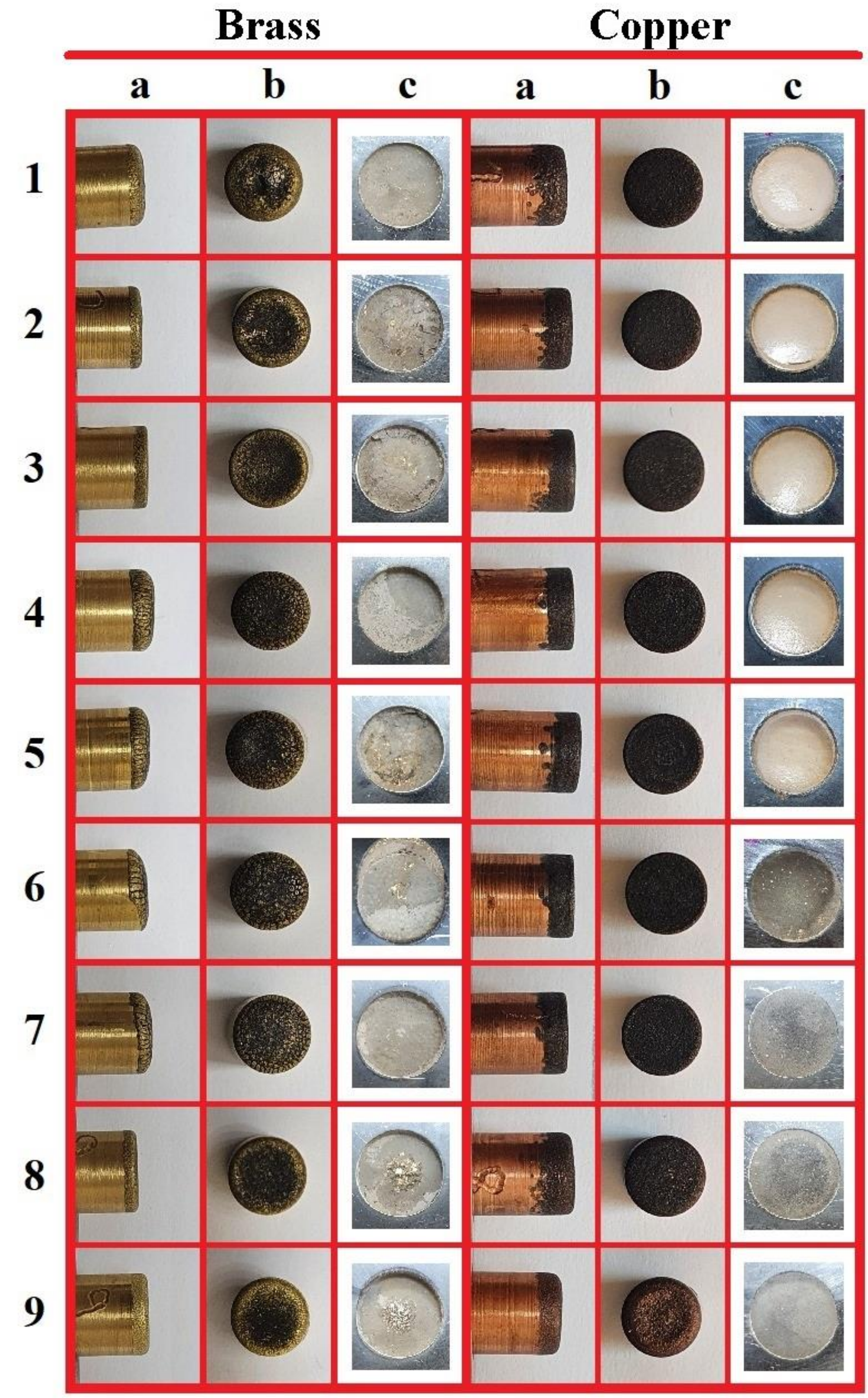

Figure 5. Processed test samples: (a) electrode side (b) electrode top (c) workpiece hole

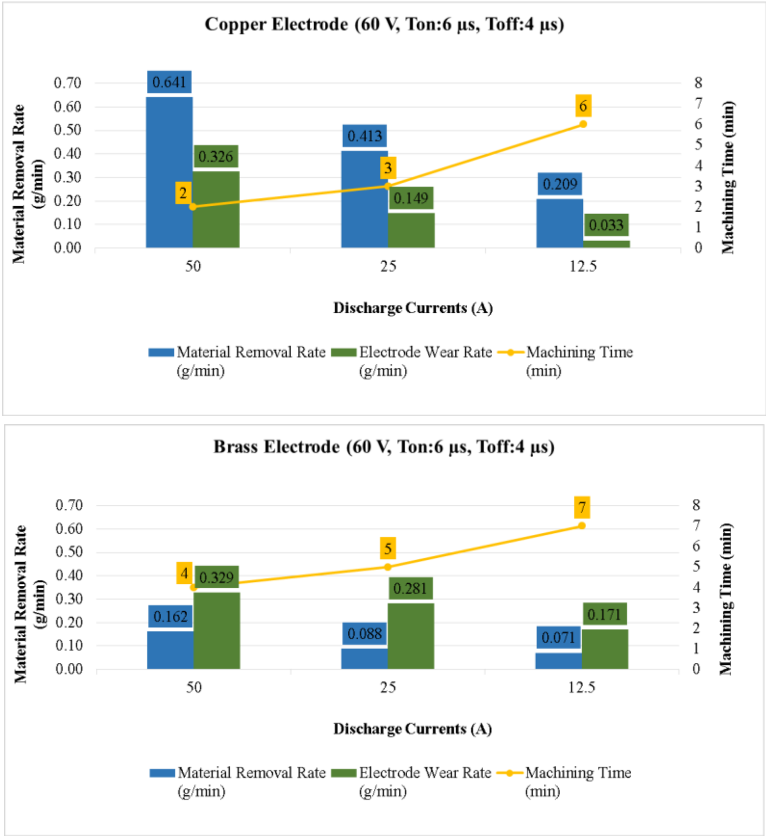

Figure 6. Material removal rate and machining times due to increased machining current

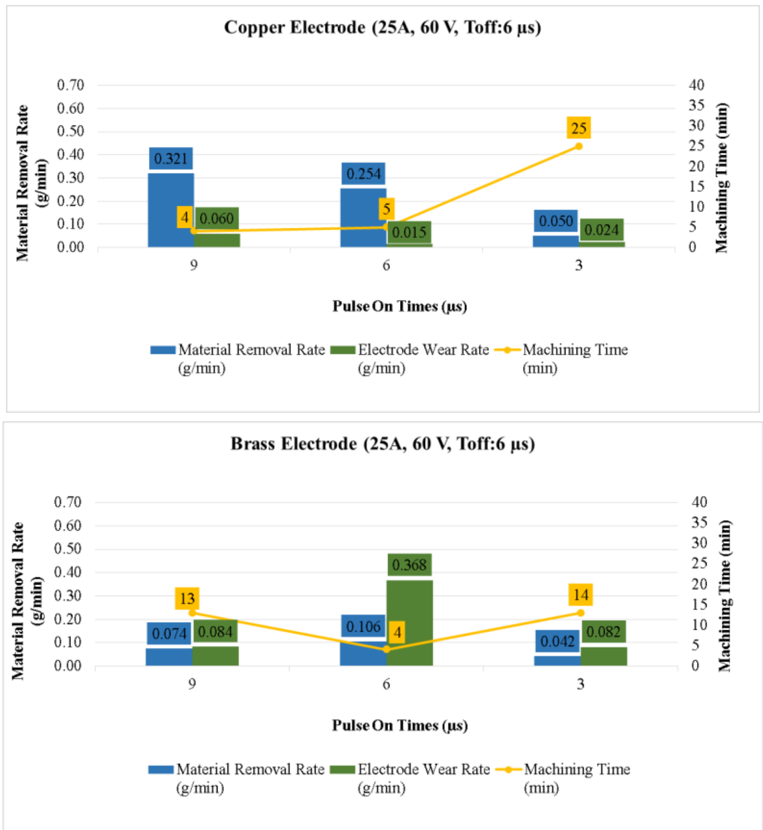

Figure 7. Material removal rate and machining times due to increased pulse on time

In the use of both copper and brass electrodes at constant voltage, pulse on times and pulse off times; as the machining current increased, the material removal rate and electrode wear rate increased and the machining time decreased due to the increased sparking between the workpiece and the electrode. Machining current was determined as the most effective parameter compared to other parameters in terms of effect on machining time, MRR and EWR. It is seen in Figure 6 that the ratios obtained are linear in copper and brass electrodes.

When the graphs in Figure 7 are examined, it is seen that the decrease in the arc duration increases the processing time in the use of both copper and brass electrodes. In Figure 7, the high thermal conductivity and thermal conductivity of the electrode led to an increase in the metal removal rate at high arc times in the use of copper electrodes. The electrode wear rate increased and the material removal rate decreased compared to copper electrodes in the use of brass electrodes since the mechanical and physical properties of the brass electrode are lower than that of copper (Pavan et al., 2021).

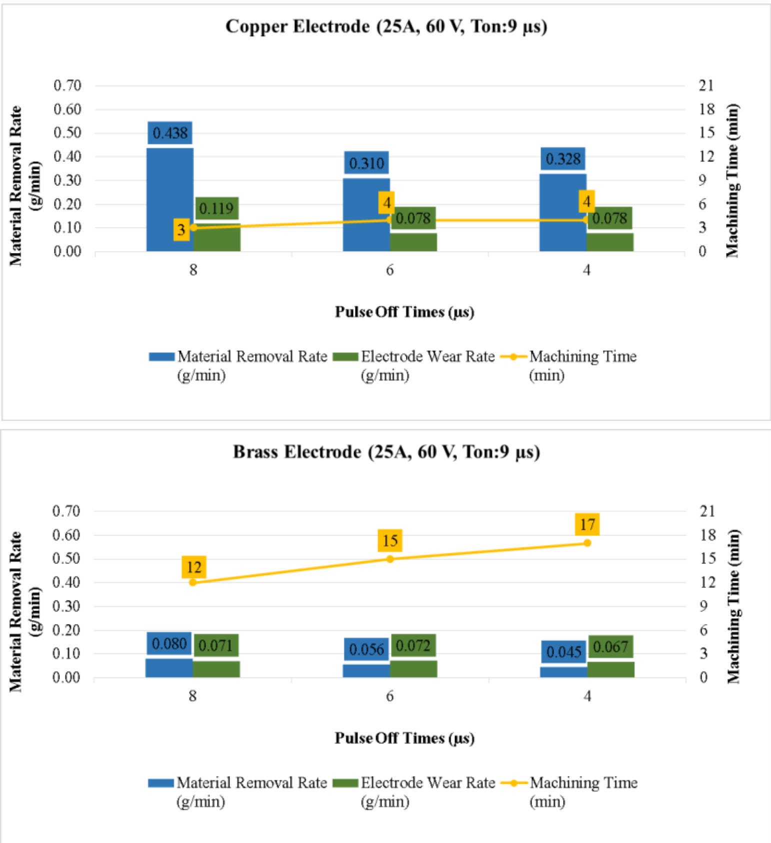

Figure 8. Material removal rate and machining times based on pulse off time

Figure 8 shows the effects of varying pules off times at constant 25A current, 60V voltage and 9µs pulse on time. The pulse off time is the period of no arcing between two pulse on times. In general, although the increase in the pulse off time increases the processing time, in this study, the MRR increased with the increase in the pulse off time, and the machining time decreased in general. The long pulse off time allowed the debris and electrode residues that spread to the environment during the arc to be evacuated successfully in the arc area with the sprayed electro-erosion liquid, both increasing the material removal rate and shortening the processing time.

In EDM, there is no mechanical contact between the electrode and the workpiece, there is a repetitive electrical discharge in a dielectric environment. As a result of the heat reaching approximately 20,000°C, melting and evaporation occur in the workpiece. No mechanical stress occurs in this process (Sengottuvel et al., 2013; Torres et al., 2017). The deformations that occur at the corners of the electrodes during EDM are mainly caused by the excessive electrical density at the electrode tip (Yıldız, 2018). This causes excessive wear on the corners of the electrodes. The form and size of the electrode material at the beginning of erosion are not the same as after EDM. For this reason, the start and end dimensions of the form on the workpiece are different. This causes the kerf angle. In Tables 11 and 12, the dimensions of the workpiece drilled with copper and brass electrodes, respectively, and the kerf angles determined on the workpiece and electrode are given. In this study, a process was applied to remove chips at a distance of 5 mm from the surface of the 3 mm thick workpiece with the EDM machine. While drilling with copper electrodes, 3 mm deep holes were obtained on the workpiece, blind holes with a depth of 1.01 – 2.30 mm were obtained in the use of brass electrodes due to electrode wear.

Table 11. Hole diameters and kerf angles of materials processed by copper electrodes

Test No	Sleipner Workpiece			Kerf (degree)	
	Hole top dia. (mm)	Hole in dia. (mm)	Depth (mm)	Hole top dia. (mm)	Hole in dia. (mm)
1	8.60	8.17	3.00	4.10	0.85
2	8.40	8.11	3.00	2.77	0.46
3	8.38	8.24	3.00	1.34	0.27
4	8.60	8.40	3.00	1.91	0.57
5	8.40	8.10	3.00	2.86	0.07
6	8.60	8.38	3.00	2.10	1.58
7	8.54	8.26	3.00	2.67	0.39
8	8.50	8.22	3.00	2.67	0.48
9	8.34	8.24	3.00	1.00	0.60

Table 12. Hole diameters and kerf angles of materials processed by brass electrodes

Test No	Sleipner Workpiece			Kerf (degree)	
	Hole top dia. (mm)	Hole in dia. (mm)	Depth (mm)	Hole top dia. (mm)	Hole in dia. (mm)
1	8.40	8.24	1.55	2.95	0.55
2	8.37	8.26	1.05	3	2.26
3	8.30	8.27	1.20	0.72	0.41
4	8.40	8.30	2.30	1.25	0.31
5	8.40	8.26	2.00	2	0.24
6	8.23	8.10	1.92	1.94	0.15
7	8.60	8.26	2.24	4.34	0.84
8	8.40	8.30	1.01	2.83	0.31
9	8.30	8.20	1.45	1.97	0.40

The comparison of the average material removal rate, electrode wear rate and machining times obtained depending on the use of copper and brass electrodes in a single graph is shown in Figure 9. These values were calculated by taking the arithmetic mean of all test results.

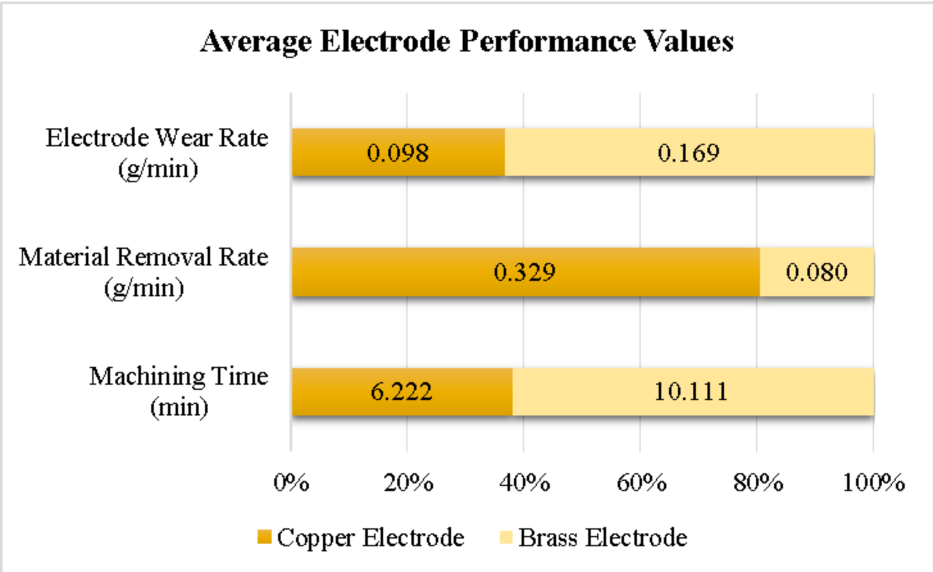

Figure 9. Performance values of Copper and Brass electrodes

In the use of copper electrodes, the metal removal rate increased by 311.25% on average, compared to the use of brass electrodes, while the electrode wear rate and machining time decreased by 42.01% and 38.46%, respectively. This can be explained by the higher thermal conductivity and electrical conductivity of the copper electrode than the brass electrode. The increase in sparking and thermal effects between the workpiece and the electrode resulted in an increase in the metal removal rate and a decrease in the machining time (Pavan et al., 2021).

4. Conclusions

•It is seen that the decrease in pulse on time increases the machining time in the use of both copper and brass electrodes. In the use of copper electrodes, the high electrical conductivity and thermal conductivity of the electrode at high pulse on time result in an increase in the MRR.

• In the use of both copper and brass electrodes at constant voltage, pulse on time and puls off time, as the machining current increases, the MRR and EWR increase and the machining time decreases due to the increased sparking between the workpiece and the electrode. Machining current is determined as the most effective parameter in terms of effect on machining time, MRR and EWR compared to other parameters.

• In general, although the increase in the pulse off time increases the machining time; in this study, the MRR increases with the increase in the pulse off time, and the machining time decreases in general. The successful evacuation of the debris and electrode residues that spread to the environment during the long pulse off time in the arc area with the sprayed electro-erosion liquid increases the MRR and shorten the processing time.

• In the use of copper and brass electrodes with different processing parameters, the inlet diameters of the drilled holes are found to be larger than the outlet diameters as well as an irregular kerf formation is observed due to debris evacuation and worn electrodes.

• In the use of copper electrodes, the metal removal rate increases by 311.25% on average, compared to the use of brass electrodes, while the electrode wear rate and machining time decrease by 42.01% and 38.46%, respectively. This can be explained by the higher thermal conductivity and electrical conductivity of the copper electrode than the brass electrode. The increase in sparking and thermal effects between the workpiece and the electrode result in an increase in the metal removal rate and a decrease in the machining time.

Acknowledgments

The author(s) received no financial support for the research, authorship, and/or publication of this article.

Authors' contributions

FC and EK designed the structure. FC fabricated the device, carried out the experiments work, the theoretical calculations, in collaboration with EK, and wrote up the article. ESG came up with the idea of the study. FC, EK and ESG contributed to the interpretation and English writing. All authors have read and approved the final version of the article.

Competing interests

The authors declare that they have no competing interests.

Refereneces

Abhishek K., Datta S., Biswal BB., Mahapatra SS. Machining performance optimization for electro-discharge machining of Inconel 601, 625, 718 and 825: an integrated optimization route combining satisfaction function, fuzzy inference system and Taguchi approach. Journal of the Brazilian Society of Mechanical Sciences and Engineering 2017; 39(9): 3499-3527.

Akbulut A., Kürşad GÖV. Micro hole drilling of aerospace materials and regression analysis. El-Cezeri Journal of Science and Engineering 2020; 7(2): 710-723.

Azad MS., Puri AB. Simultaneous optimisation of multiple performance characteristics in micro-EDM drilling of titanium alloy. The International Journal of Advanced Manufacturing Technology 2012; 61(9): 1231-1239.

Ceritbinmez F., Kanca E. The effects of cutting parameters on the kerf and surface roughness on the electrode in electro erosion process. Gazi University Journal of Science Part C: Design and Technology 2021; 9 (2): 335-346.

Ceritbinmez F., Yapıcı A. Investigation of the effect of processing parameters on kerf and surface roughness in the machining of Sleipner cold work tool steel with copper chromium zirconium alloy electrode in electro-erosion machine. The Black Sea Journal of Sciences 2021; 11(2): 570-583.

Dhanabalan S., Sivakumar K., Narayanan CS. Experimental investigation on electrical discharge machining of titanium alloy using copper, brass and aluminum electrodes. Journal of Engineering Science and Technology 2015; 10(1): 72-80.

D'Urso, G., Maccarini, G., & Ravasio, C., Influence of electrode material in micro-EDM drilling of stainless steel and tungsten carbide. The International Journal of Advanced Manufacturing Technology 2016; 85(9), 2013-2025.

Engin, N. A. S., Argun, K., & Zurnacı, E., Invesigation of effect on surface roughness of parameters at machining with graphide electrode in EDM of AISI 1.2738 Steel. Düzce University Journal of Science and Technology 2018; 6(4), 1082-1093.

https://www.uddeholm.com/tr/products/uddeholm-sleipner/ (Erişim 30.04.2022)

https://www.saglammetal.com/en/copper/hard-copper-alloys/cupro-max-cucrzr (Erişim 30.04.2022)

https://www.saglammetal.com/tr/bronz/pirincler/cuprass-cuznal (Erişim 30.04.2022)

Joshi A., Saraf AK., Goyal RK. EDM machining of die steel EN8 and testing of surface roughness with varying parameters. Materials Today: Proceedings 2020; 28, 2557-2560.

Kirkhorn L., Frogner, K., Andersson, M., Ståhl JE. Improved tribotesting for sheet metal forming. Procedia CIRP 2012; 3, 507-512.

Kuppan P., Rajadurai A., Narayanan S. Influence of EDM process parameters in deep hole drilling of Inconel 718. The International Journal of Advanced Manufacturing Technology 2008; 38(1): 74-84.

Mahajan R., Krishna H., Singh AK., Ghadai RK. A review on copper and its alloys used as electrode in EDM. In IOP Conference Series: Materials Science and Engineering 2018; 377(1):. 012183.

Mouralová K., Bednar J., Benes L., Hrabec P., Kalivoda M., Fries J. The analysis of EDM electrodes wear in corners and edges. Archives of Civil and Mechanical Engineering 2020; 20(4): 1-14.

Niamat M., Sarfraz S., Shehab E., Ismail SO., Khalid QS. Experimental characterization of electrical discharge machining of aluminum 6061 T6 alloy using different dielectrics. Arabian Journal for Science and Engineering 2019; 44(9): 8043-8052.

Pantazopoulos G., Psyllaki P., Kanakis D., Antoniou S., Papadimitriou K., Sideris J. Tribological properties of a liquid nitrocarburised special purpose cold work tool steel. Surface and Coatings Technology 2006; 200(20-21): 5889-5895.

Pavan C., Sateesh N. Taguchi analysis on machinability of Inconel 600 using copper, brass, and copper tungsten electrodes in EDM. Materials Today: Proceedings 2021; 46, 9281-9286.

Payal HS., Choudhary R., Singh S. Analysis of electro discharge machined surfaces of EN-31 tool steel 2008.

Quarto M., D'Urso G., Giardini C., Maccarini G. FEM model development for the simulation of a micro-drilling EDM process. The International Journal of Advanced Manufacturing Technology 2020; 106(7): 3095-3104.

Raj S., Sinha HR., Das S., Guha S., Banik D., Routara BC. Optimization of surface topography of electro-discharge machined super alloy ınconel 825: using TOPSIS ıntegrated with taguchi philosophy. Materials Today: Proceedings 2020; 24, 218-224.

Rajesha S., Sharma AK., Kumar P. On electro discharge machining of Inconel 718 with hollow tool, Journal of Materials Engineering and Performance 2012; 21(6): 882-891.

Sahu AK., Mahapatra SS. Surface characteristics of EDMed titanium alloy and AISI 1040 steel workpieces using rapid tool electrode. Arabian Journal for Science and Engineering 2020; 45(2:, 699-718.

Sengottuvel P., Satishkumar S., Dinakaran D. Optimization of multiple characteristics of EDM parameters based on desirability approach and fuzzy modeling. Procedia Engineering 2013; 64, 1069-1078.

Shu KM., Shih HR., Tu GC. Electrical discharge abrasive drilling of hard materials using a metal matrix composite electrode. The International Journal of Advanced Manufacturing Technology 2006; 29(7): 678-687.

Skrabalak G. Influence of electrode tool length on the micro EDM drilling performance. Procedia CIRP 2018; 68, 594-598.

Soydan O., Göv K., Eyercioğlu Ö. Surface finishing of aerospace materials. El-Cezerî Journal of Science and Engineering 2020; 7(2): 700-709.

Tawfiq MA., Abbas AA.. Effect of current and pulse on time on MRR an EWR for different inner electrode shape of EDM process. Global Journal of Engineering Science and Research Management 2018; 5(8): 13–26.

Torres A., Puertas I., Luis CJ. EDM machinability and surface roughness analysis of INCONEL 600 using graphite electrodes. The International Journal of Advanced Manufacturing Technology 2016; 84(9): 2671-2688.

Yıldız Y. Die-sinking electrical discharge machining of magnesium-calcium (Mg0.8Ca) alloy for biomedical applications. Dokuz Eylul University-Faculty of Engineering Journal of Science and Engineering 2018; 20(59): 336-346.